Acta Materialia 115 (2016) 76–82

Contents lists available at ScienceDirect

Acta Materialia

journal homepage: www.elsevier.com/locate/actamat

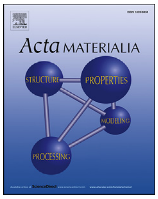

Full length article

Size and orientation dependent mechanical behavior of body-centered tetragonal Sn at 0.6 of the melting temperature

Bastian Philippi [a, *], Christoph Kirchlechner [a, b], Jean Sébastien Micha [c], Gerhard Dehm [a, **]

[a] *Max-Planck-Institut für Eisenforschung GmbH, Max-Planck-Straße 1, 40237 Düsseldorf, Germany*
[b] *Department of Materials Physics, Montanuniversität Leoben, Franz Josef-Straße 18, 8700 Leoben, Austria*
[c] *University Grenoble Alps, CEA-Grenoble, Institut Nanosciences et Cryogénie, rue des Martyrs 17, 38054 Grenoble, France*

ARTICLE INFO

Article history:
Received 4 April 2016
Received in revised form
24 May 2016
Accepted 30 May 2016

Keywords:
Tin
Sn
Micromechanics
Size-effect
Synchrotron diffraction
Plasticity
Lead-free solder

ABSTRACT

Although, tin is one of the most prominent metals in soldering, very little is known about its mechanical behavior. In addition, possible size-effects of tin can become restricting for the ongoing miniaturization of microelectronic devices. Due to the low melting temperature of 505.15 K and the body-centered tetragonal crystal structure, differences in the mechanical behavior compared to face-centered cubic and body-centered cubic metals can be expected. Since Tin is especially interesting because of its multiple different slip systems, post mortem slip step analysis allowed to determine the activated slip systems and thus, to calculate size dependent critical resolved shear stresses. The measured size scaling exponent (-1.07 ± 0.06) is close to model-predictions of -1, irrespective of the activated families of slip systems in different orientations. Furthermore, an exceptional low scatter of the flow stress in various samples and no apparent hardening is found. It is concluded, that the activation of dislocation sources instead of dislocation-dislocation interactions are responsible for the observed behavior. This is in line with complementary μLaue diffraction experiments which indicate an unresolvable low density of geometrical necessary dislocations.

1. Introduction

While Tin is one of the main components in the legislation-driven development of non-hazardous lead-free solder materials [1], the understanding of its mechanical behavior is lagging behind the immense reliability demand in electronic materials. Especially, the size dependence of the mechanical behavior is of great importance with respect to the ongoing miniaturization in the large field of microelectronics.

In the past decade, micromechanical testing of single crystalline materials revealed, that a size effect of the flow stress occurs regularly in a multitude of experiments for face-centered cubic (fcc), body-centered cubic (bcc) and hexagonal materials [2–4]. The size effect is expressed by an increased flow stress with reducing sample size [5], as well as an intrinsic scatter of the yield strength. The size scaling has often been described by a power-law dependence [2] exhibiting a scaling exponent ranging from -0.8 up to -0.2 for fcc (e.g. Au, Ni & Cu [6–8]) and bcc (e.g. Mo, Ta, Nb & W [4,9]) metals. In spite of sustained efforts undertaken by multiple groups to understand this behavior, still no unified mechanism, capturing all aspects of the size effect, has been published yet. Moreover, deviations between exponents predicted by the existing models and experiments cannot be explained satisfactory.

The unique properties of Tin in terms of a low melting temperature (T_m) at 505.15 K [11] along with a body-centered tetragonal (bct) crystal structure, allow a complementary approach to fcc and bcc materials in studying mechanical behavior and size effects at high (0.58 T_m) homologous temperatures i.e. ratio of testing temperature and absolute melting temperature in materials with distinct plastic anisotropy.

Due to the pronounced tetragonality of the unit cell (c/a ratio of 0.5457 [12]), Sn is expected to show several families of possible slip systems as listed in Table 1. Microscopic analysis of tensile tested samples revealed inconsistent and contradictory results as reviewed by Yang et al. [13]. Hence, the calculation of effective critical resolved shear stress (CRSS) values from measured data hasn't been covered satisfactory so far. Only density functional theory (DFT) computations were used to predict CRSS but

---

* Corresponding author.
** Corresponding author.
E-mail addresses: philippi@mpie.de (B. Philippi), dehm@mpie.de (G. Dehm).

http://dx.doi.org/10.1016/j.actamat.2016.05.055
1359-6454/

Table 1
Possible slip system families observed by different sources. Note that only [100] and [010] crystal directions produce interchangeable permutations in contrast to the shorter [001] direction.

Slip plane	Slip direction	Source
{110}	$\langle\bar{1}11\rangle$	[12,23]
{110}	$\langle 001\rangle$	[12,33]
{100}	$\langle 010\rangle$	[12,23,34]
{100}	$\langle 001\rangle$	[33]
{101}	$\langle\bar{1}01\rangle$	[33]
{121}	$\langle\bar{1}01\rangle$	[33]
{100}	$\langle 011\rangle$	[35,36]
{101}	$\langle 11\bar{1}\rangle$	[35,36]
{101}	$\langle 010\rangle$	[35,36]
{001}	$\langle 100\rangle$	[35,36]
{001}	$\langle 110\rangle$	[35,36]
{121}	$\langle 1\bar{1}1\rangle$	[35,36]

experimental validation is still needed [14].

Thus, this study aims to unravel the size-dependent CRSS of tin for different orientations by means of micro-pillar compression tests [10] at 0.58 homologous temperature.

2. Experimental details

In order to investigate the size-dependent mechanical behavior of Sn, *in situ* micromechanical testing was conducted on single-crystalline specimens in form of micro-pillar compression tests in a scanning electron microscope (SEM) accompanied by post mortem synchrotron based Laue microdiffraction (μLaue) experiments.

The micro-samples were prepared from commercially available, cylindrical shaped single crystals of β-Sn with an [001] and [110] crystal oriented along the growth direction, provided by MaTecK GmbH (Jülich, Germany). As a first step a rectangular piece was cut along the chosen orientation with respect to the cylinder axis by spark erosion with dimensions of about 10 mm width, 3 mm height and 0.5 mm thickness. For the fabrication of the micro-samples the approach of Moser et al. [15] was carried out: Diamond wire saw cutting was used to further reduce the sample size to generate lamellae with small dimensions allowing electrochemical etching (2 mm width, 3 mm height and 0.5 mm thickness). During electrochemical thinning the lamellae were periodically dipped into a Struers (Willich, Germany) A2 electrolyte, while a potential of 18 V was applied. By protecting the lower part and sides of the sample with Lacomit® varnish a stable base was generated while the exposed surface on the top (facing the indenter) was polished and thinned down to 20–50 μm thickness on the upper edge, reducing the required amount of focused ion beam (FIB) machining significantly. Afterwards the lamellae were glued onto homebuilt sample holders, suitable for all applied indentation devices or microscope stages to ensure that the selected orientation is maintained during all following preparation steps and experiments. In the last preparation step, FIB milling was carried out in a Zeiss® Auriga dual-beam system to machine the electrochemically thinned edge of the lamella into around 10 micro-pillars per lamella with several size ranges between 1 and 10 μm and an aspect ratio (length/width) of 3:1. Rectangular shaped pillars with constant cross-section along the pillar height were machined with beam currents of 4 nA at 30 kV for coarse milling, while subsequent fine milling was carried out with 600 pA and finally 120 pA at 30 kV. For reference, bulk compression samples of 6 mm diameter and 8 mm height were prepared for both orientations from the same single crystals by spark erosion.

To determine the actual pillar orientation electron backscatter diffraction (EBSD) measurements were conducted with an EDAX®/TSL® detector setup with a Hikari® charged coupled device (CCD) camera.

The mechanical compression tests were conducted in a JEOL® JSM6349 SEM for *in situ* observations and accurate alignment, loading the micro-pillars with an ASMEC UNAT 2 (Asmec GmbH, Radeberg, Germany) nanoindenter. All experiments were performed in displacement controlled open loop mode with a loading rate of 10^{-4} s^{-1} and up to a maximum strain of 30%. In order to prevent heavy barreling, most pillars were compressed to significantly lower strains then this maximum value to ensure a reliable stress evaluation. Several intermediate unloadings were carried out to carefully analyze the quality of micro-pillar to flat-punch alignment and to reduce the impact of lateral constraints [16]. The activated slip systems were analyzed in a field emission gun SEM after the deformation.

To ensure comparability, the bulk compression testing was conducted with a Schenck Trebel universal testing machine at the same loading rate of 10^{-4} s in displacement controlled mode.

Post mortem μLaue investigations were performed at the μLaue station of the French CRG-IF beamline at the bending magnet synchrotron source BM32 [17] of the European synchrotron radiation facility (ESRF). The spectral width of the beam ranges from 5 to 22 keV while it is laterally focused to roughly 300 × 500 nm^2 by a set of Kirkpatric-Baez (KB) mirrors. Consequently information of a single pattern originates from a rectangular shaped rod with a penetration depth of 7 μm without significant attenuation for most measured peaks. The Laue patterns were recorded by a 2048 × 2048 pixel Rayonix camera with an exposure time of 0.1 s, followed by a readout of around 6 s. An unstrained Germanium (100) wafer and XMAS software package were used for geometrical calibration and peak indexation [18]. Sample positioning was assisted by optical microscope and x-ray fluorescence imaging using Sn-K_α with submicron resolution according to [19]. Post-deformation mesh scans of 30 × 30 μm^2 with a step size of 1 μm were used to scan the entire sample. From the indexed Laue patterns the point to origin misorientation angle was calculated.

3. Results and interpretation

3.1. In situ compression testing in SEM

The compression of different sized [110]-oriented pillars, with

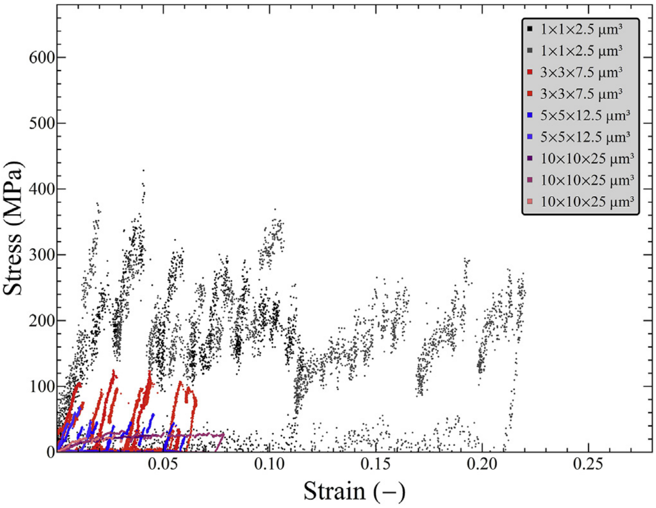

Fig. 1. Stress-strain curves for 1, 3, 5 and 10 μm sized pillars oriented in [110], showing the size dependence of the flow stress and absence of hardening.